Nonlin. Processes Geophys. Discuss., doi:10.5194/npg-2016-68, 2017
Manuscript under review for journal Nonlin. Processes Geophys.
Published: 13 January 2017
© Author(s) 2017. CC-BY 3.0 License.

Nonlinear Processes in Geophysics
Discussions
Open Access
EGU

Impact of Optimal Observational Time Window on Coupled Data Assimilation: Simulation with a Simple Climate Model

Yuxin Zhao[1], Xiong Deng[1,3], Shaoqing Zhang[2], Zhengyu Liu[4,5], Chang Liu[1,3], Gabriel Vecchi[6], Guijun Han[7], Xinrong Wu[7]

[1]College of Automation, Harbin Engineering University, Harbin, 150001, China
[2]Key Laboratory of Physical Oceanography, MOE.China, Ocean University of China, Qingdao, 266003, China
[3]NOAA/GFDL-University of Wisconsin-Madison Joint Visiting Program, Princeton, NJ08540, USA
[4]Laboratory for Climate and Ocean-Atmosphere Studies (LaCOAS), Department of Atmospheric and Oceanic Sciences, School of Physics, Peking University, Beijing, 100871, China
[5]Center for Climate Research and Department of Atmospheric and Oceanic Sciences, University of Wisconsin-Madison, Madison, WI 53706, USA
[6]NOAA/GFDL, Princeton, NJ08540, USA
[7]National Marine Data and Information Service, Tianjin, 300171, China

Correspondence to: Shaoqing Zhang (Shaoqing.Zhang@noaa.gov)

Abstract. Climate signals are the results of interactions of multiple time scale media such as the atmosphere and ocean in the coupled earth system. Coupled data assimilation (CDA) pursues balanced and coherent climate analysis and prediction initialization by incorporating observations from multiple media into a coupled model. In practice, an observational time window (OTW) is usually used to collect measured data for an assimilation cycle to increase observational samples. Given different time scales of characteristic variability in different media, what are the optimal OTWs for the coupled media so that climate signals can be most accurately recovered by CDA? With a simple coupled model that simulates typical scale interactions in the climate system, we address this issue here. Results show that required by retrieval of characteristic variability of each coupled medium, an optimal OTW determined from the de-correlation time scale provides maximal observational information that best fits characteristic variability of the medium during the data blending process. Maintaining correct scale interactions, the resulted CDA improves the analysis of climate signals greatly. The simple model results provide a guideline when the real observations are assimilated into a coupled general circulation model for improving climate analysis and prediction initialization by accurately recovering important characteristic variability such as sub-diurnal in the atmosphere and diurnal in the ocean.

1 Introduction

Currently, the interactions between the earth climate system's major components, such as the atmosphere, ocean, land and sea ice, have been reasonably simulated by the coupled climate models, which can also give the evaluation of climate changes (Randall et al. 2007). However, because of the uncertainties and errors in models (e.g., parameterization is only an approximation and dynamical core is imperfect), models always tend to produce different climate features and variability

Nonlin. Processes Geophys. Discuss., doi:10.5194/npg-2016-68, 2017
Manuscript under review for journal Nonlin. Processes Geophys.
Published: 13 January 2017
© Author(s) 2017. CC-BY 3.0 License.

from the real world (e.g. Delworth et al. 2006; Collins et al. 2006; Zhang et al. 2014). Due to the significant importance of preserving the balance and coherence of different model components (or media) during the coupled model initialization, data assimilation for state estimation and prediction initialization should be performed within a coupled climate model framework (e.g. Chen et al. 1995; Zhang et al. 2007; Chen 2010; Han et al. 2013). The characteristic variability time scales of different media within the coupled climate model frameworks are usually different. When the observation data including in one or more components of the coupled system framework are assimilated, the observational information will be able to transfer among different media through the coupled dynamics so that all media gain consistent and coherent adjustments. Such an assimilation procedure is called coupled data assimilation (CDA), which can sustain the nature of multiple time-scale interactions during climate estimation and prediction initialization (e.g. Zhang et al. 2007; Sugiura et al. 2008), thus producing better climate analysis and prediction initialization and therefore improve the coupled models' predictability (e.g. Yang et al. 2013).

During the coupled data assimilation in each medium, here an observational time window (OTW) is used to collect measured data for an assimilation cycle (e.g. Pires et al., 1996; Hunt et al., 2004; Houtekamer and Mitchell, 2005; Laroche et al., 2007) to increase observational samples centred at the assimilation time. This assumes that all the collected data sample the "truth" variation at the assimilation time (Hamill and Snyder 2000; Zhang et al. 2011; Gao et al. 2013). Apparently, while a large OTW provides more observational samples at the assimilation time, the assimilation process blends more data from different times and may distort variability being retrieved. Given the fact that climate signals are the results of interactions of multiple time scale media, correct variability retrieved for each medium so as correct scale interaction maintained in CDA is particularly important for climate analysis and prediction initialization. In this study we attempt to answer the following two questions: 1) For each coupled component within the coupled model framework, whether or not exist an optimal OTW so that the assimilation fitting has maximum observational information but minimum variability distortion? 2) What's the impact of optimal OTWs on the quality of CDA for climate estimation and prediction initialization?

With a simple conceptual coupled climate model and a sequential implementation of the ensemble Kalman filter, this study first identify the optimal OTW for each coupled medium with analysing the characteristic variability time scale of that. Then the optimal OTWs' impact on the quality of CDA and its linkage with the corresponding time scale of characteristic variability/ de-correlation are investigated. The simple coupled model consists of three typical components, including the synoptic atmosphere (Lorenz 1963) and the seasonal-interannual slab upper ocean (Zhang et al. 2012) coupling with the decadal deep ocean (Zhang 2011a,b). Although the simple conceptual coupled model does not share the similar complex physics with a coupled general circulation model (CGCM), it does reasonably simulates the typical interactions between multiple time-scale components in the coupled climate system. (Zhang et al. 2013). The simple coupled model helps us understand the essence of the problem by revealing the relationship between the optimal OTWs and corresponding time scales of characteristic variability as well as their impact on CDA. The low-cost nature of the simple model also provides convenience for a large number of CDA experiments with different OTWs in optimal OTW detection. The ensemble filter (e.g. Evensen 1994; 2007; Whitaker and Hamill 2002; Anderson 2001; 2003) used in this study is the ensemble adjustment

Nonlin. Processes Geophys. Discuss., doi:10.5194/npg-2016-68, 2017
Manuscript under review for journal Nonlin. Processes Geophys.
Published: 13 January 2017
© Author(s) 2017. CC-BY 3.0 License.

Kalman filter (EAKF, e.g. Anderson 2001; 2003; Zhang and Anderson 2003). Using the EAKF with the simple coupled model, we first establish a twin experiment framework. Within such a framework, the degree by which the state estimation based on a certain OTW recovers the truth is an assessment of the influence of the OTW on the quality of CDA. By such a way, the optimal OTW of each medium is detected and the impact of optimal OTWs on CDA is evaluated. We also discuss the influence of model bias on optimal OTW through biased twin experiment setting.

This paper is organized as follows. Section 2 briefly describes the simple conceptual coupled model, the ensemble adjustment Kalman filter, as well as the twin experiment framework including perfect and biased settings. With a simplest case, we first show the influence of OTWs on assimilation quality and its linkage with the time scale of characteristic variability/de-correlation in section 3. Then section 4 presents results on detection of the optimal OTWs for different media and the impact of optimal OTWs on CDA. The influence of realistic assimilation scenarios on optimal OTWs is discussed in section 5. Finally, summary and discussions are given in section 6.

2 Methodology

2.1 The model

Due to the complicate physical processes and huge computational cost involved, using a CGCM will be very inconvenient to investigate the impact of the different OTWs on the analysis of climate signals so as to detect each coupled medium's optimal OTW. Instead, here we employ a simple coupled "climate" model developed by Zhang (2011a). This simple model is based on the Lorenz's 3-variable chaotic model (Lorenz 1963) that couples with a slab upper ocean (Zhang et al. 2012) and a simple pycnocline predictive model (Gnanadesikan 1999). Although very simple and low computational cost, in terms of multi-scale interaction inducing low-frequency climate signals, this model shares fundamental character with a CGCM and very suitable for addressing the problem that is concerned here. And for the readers' convenience, here we simply review the physical processes involved in this conceptual coupled model. The governing equations with all quantities being given in non-dimensional units are:

$$\begin{aligned}
\dot{\mathcal{X}}_1 &= -\sigma\mathcal{X}_1 + \sigma\mathcal{X}_2 \\
\dot{\mathcal{X}}_2 &= -\mathcal{X}_1\mathcal{X}_3 + (1+\mathcal{C}_1\omega)k\mathcal{X}_1 - \mathcal{X}_2 \\
\dot{\mathcal{X}}_3 &= \mathcal{X}_1\mathcal{X}_2 - b\mathcal{X}_3 \\
\mathcal{O}_m\dot{\omega} &= \mathcal{C}_2\mathcal{X}_2 + \mathcal{C}_3\eta + \mathcal{C}_4\omega\eta - \mathcal{O}_d\omega + \mathcal{S}_m + \mathcal{S}_s\cos(2\pi t/\mathcal{S}_{pd}) \\
\Gamma\eta &= \mathcal{C}_5\omega + \dot{\mathcal{C}}_6\omega\eta - \mathcal{O}_d\eta
\end{aligned} \tag{1}$$

where $\mathcal{X}_1, \mathcal{X}_2 \text{and} \mathcal{X}_3$ represent the atmospheric model states while ω and η denote those for upper and deep ocean, respectively. A dot above the variable denotes the time tendency. The atmosphere model states are the high frequent variables while the slab oceanic variable is of a lower frequency. For sustaining the chaotic nature of the atmosphere in reality, the standard values of the parameters including in the atmospheric component (σ, k and b) are set as 9.95,28 and 8/3, respectively. In the equation of ω, the parameters $\mathcal{O}_d$ and $\mathcal{O}_m$ denote the damping coefficient and heat capacity of the upper

Nonlin. Processes Geophys. Discuss., doi:10.5194/npg-2016-68, 2017
Manuscript under review for journal Nonlin. Processes Geophys.
Published: 13 January 2017
© Author(s) 2017. CC-BY 3.0 License.

slab ocean, respectively. Due to the lower frequency of ω than that of the model states in the atmospheric components, the time scale of the upper slab ocean variables must be much slower than that of the atmospheric model states. Thus the damping rate parameter ($\mathcal{O}_d$) should be much smaller than the heat capacity, namely $\mathcal{O}_d \ll \mathcal{O}_m$. Here we define the atmospheric time scale as ~O(1) and set the parameters $(\mathcal{O}_m, \mathcal{O}_d)$ as (10,1), which show that the slab oceanic variables' time scale is ~O(10), 10 times of that of the atmospheric model states. While the $\mathcal{S}_m + \mathcal{S}_s \cos(2\pi t/\mathcal{S}_{pd})$ represents the external forcing, the parameter $\mathcal{S}_{pd}$ denoting the model seasonal cycle is set as 10 to make sure that the period of the external forcing is comparable with the upper slab ocean variables' time scale. Namely in this simple coupled model, the seasonal cycle is set as 10TUs and thus a model year (decade) equals to 10 (100)TUs. And the parameter $\mathcal{S}_s$ and $\mathcal{S}_m$, denoting the magnitudes of the external forcing's seasonal cycle and annual mean, are insensitive to the coupled model and set as (1,10). The coefficients $\mathcal{C}_1$and $\mathcal{C}_2$ in the equations of $\mathcal{X}_2$and ω are used to implement the coupling between the fast atmospheric model states and upper slab oceanic variables and set as (0.1,1), with that $\mathcal{C}_1$ denotes the upper slab oceanic forcing on the atmosphere while $\mathcal{C}_2$ in contrast. In addition, $\mathcal{C}_3$ and $\mathcal{C}_4$represent the deep oceanic forcing and the nonlinear interaction between the upper and deep ocean. And in order to make sure that the atmospheric forcing plays a dominant role in the upper slab ocean model, the magnitudes of $\mathcal{C}_3$ and $\mathcal{C}_4$should be lower than that of $\mathcal{C}_2$and both set as 0.01. Same as Zhang (2011a), the deep ocean model state variable η, denoting the anomaly of pycnocline depth in the deep ocean, is derived from the two-term balance model of the zonal-time mean pycnocline (Gnanadesikan, 1999). Where the parameter Γ keeps as a constant while the ratio of Γ and $\mathcal{O}_d$ denotes the deep oceanic variables' time scale. Because the deep oceanic variable's time scale is slower than that of slab ocean, here it is defined as ~O(100), namely Γ is set as 100. Similar to the equation of ω, the coefficients $\mathcal{C}_5$ and $\mathcal{C}_6$denote the linear slab oceanic forcing and the nonlinear interaction between upper and deep ocean. Also for guaranteeing that the linear interaction is dominant and the nonlinear interaction is weaker than that in the deep ocean model, $\mathcal{C}_5$ and $\mathcal{C}_6$ are set as (1, 0.001). Summarily, in this study the standard values of the parameters including in this simple model $(\sigma, k, b, \mathcal{C}_1, \mathcal{C}_2, \mathcal{O}_d, \mathcal{O}_m, \mathcal{S}_m, \mathcal{S}_s, \mathcal{S}_{pd}, \Gamma, \mathcal{C}_3, \mathcal{C}_4, \mathcal{C}_5, \mathcal{C}_6)$ are set as (9.95,28,8/3,0.1,1,1,10,10,1,10,100,0.01, 0.01,1,0.001) (e.g., Zhang 2011a,b; Zhang et al., 2012; Han et al., 2013,2014).

Similar to the study of Han et al (2014), the fourth-order Runger-Kutta (RK4) time-differencing scheme is used in this paper to resolve this simple coupled model, which can be written as following Eq.(2). Where $k_0 - k_3$ denote the four time levels and Δt is the time step with $\Delta t = 0.01$TU. And φ represents state variables while $\mathcal{F}$ denotes the right term of that in Eq.(1).

$$
\begin{aligned}
k_0 &= \Delta t \mathcal{F}(t_i, \varphi^n) \\
k_1 &= \Delta t \mathcal{F}(t_i + \Delta t/2\,, \varphi^n + k_0/2) \\
k_2 &= \Delta t \mathcal{F}(t_i + \Delta t/2, \varphi^n + k_1/2) \\
k_3 &= \Delta t \mathcal{F}(t_i + \Delta t, \varphi^n + k_2) \\
\varphi^{n+1} &= \varphi^n + \tfrac{1}{6}(k_0 + 2k_1 + 2k_2 + k_3)
\end{aligned}
\qquad (2)
$$

Zhang (2011b) illustrated that, given the model parameters described above, the constructed simple coupled model can effectively simulate a fundamental feature of the real world climate system in which different time scales interact with each other to develop climate signals. In this simple conceptual coupled model, the synoptic to decadal time-scale signals are

Nonlin. Processes Geophys. Discuss., doi:10.5194/npg-2016-68, 2017
Manuscript under review for journal Nonlin. Processes Geophys.
Published: 13 January 2017
© Author(s) 2017. CC-BY 3.0 License.

produced by the interactions between the transient atmosphere attractor, the slow slab ocean and the even-slower deep ocean (see Zhang 2011a; Han et al. 2014). Again, although the simple coupled model does not have complex physics and cannot consider the impact of localization and imbalance as a CGCM, it can help us investigate the fundamental issue we want to address here more directly and clearly.

2.2 Ensemble coupled data assimilation

In the words of Zhang (2011a), during the state estimation, the error statistics evaluated from ensemble model integrations, such as the error covariance between model states, will be used in an ensemble filter to extract observational information to adjust the model states. (e.g., Evensen, 1994, 2007; Anderson, 2001; Hamill et al., 2001; Zhang, 2011a,b; Zhang et al., 2012; Han et al., 2014). In this study, a derivative of Kalman filter (Kalman 1960; Kalman and Bucy 1961) called ensemble adjustment Kalman Filter (EAKF, Anderson 2001; 2003; Zhang and Anderson 2003; Zhang et al. 2007) which is a sequential implementation of ensemble Kalman Filter under an "adjustment" idea is used to implement the CDA scheme. While the assumption of observational errors' independence allows the EAKF to sequentially assimilate observations into corresponding model states (Zhang and Anderson 2003; Zhang et al. 2007), which is of much computational convenience for data assimilation, the EAKF can maintains much the non-linearity of background flows as much as possible (e.g., Anderson, 2001; 2003; Zhang and Anderson, 2003).

Based on the two-step implementation of EAKF scheme (Anderson, 2001; 2003), firstly the observational increment (see Eqs.(2)-(5) in Zhang et al. (2007)) will be computed using

$$\Delta y_{k,i} = \left(\bar{y}_k^{u} + \Delta\acute{y}_{k,i}\right) - y_{k,i}^{p} \quad (3)$$

where $\Delta y_{k,i}$ denotes the observational increment of the ith ensemble member of the kth observation $y_{k,i}$ while $\Delta\acute{y}_{k,i}$ is updated ensemble spread of that. $y_{k,i}^{p}$ is the ith prior ensemble member of the kth observation and $\bar{y}_k^{u}$ represents the posterior mean. Once the observational increment above is obtained, the following uniform linear regression formula will be used to project that onto related model state variables:

$$\Delta z_{k,i} = \frac{c(z^{p}, y_k)}{\sigma_k^2}\Delta y_{k,i} \quad (4)$$

Where $\Delta y_{k,i}$ represents the observational increment obtained as above and $c(z^{p}, y_k)$ defines the error covariance between the prior ensemble of the model state and the model estimated observation ensemble. σ_k is the standard deviation of the model estimated ensemble of y_k. The term $\Delta z_{k,i}$ is the contribution of the kth observation to ith ensemble member of the model state estimated. When the relative observations are available, the Eq.(4) will be applied to implement CDA for state estimation in a straight forward manner (Zhang et al., 2007; Zhang 2011a;).

Although many sophisticated algorithms of the inflation scheme (e.g. Anderson 2007;2009; Li et al. 2009; Miyoshi 2011) exist for atmosphere data assimilation, the inflation scheme for a coupled model is a new subject due to the multiple time-scale nature of the system. Furthermore, trial-and-error experiments show that the usual form of inflation (e.g. only inflate the atmosphere model states or inflate all the model states equally) will lead the analysis to become unstable. Thus, in this

Nonlin. Processes Geophys. Discuss., doi:10.5194/npg-2016-68, 2017
Manuscript under review for journal Nonlin. Processes Geophys.
Published: 13 January 2017
© Author(s) 2017. CC-BY 3.0 License.

paper, for simplicity and computational convenience as well as convenience for comparison, no inflation is used in our assimilation experiments, just as in Han et al. (2014).

The ensemble initial condition is produced by adding a Gaussian white noise with the same standard deviations as observational errors (2 for X_1, X_2 and X_3, and 0.5 for ω) to the model states at the end of spin-up described next. We also choose the model states between 9000TUs and 10000TUs at an interval of 50TUs being perturbed to form 20 cases of ensemble initial conditions for each experiment analysed in section 4 and 5. In this way we attempt to minimize the dependence of the results on optimal OTW on initial states. We will analyse the mean value of 20 cases and the uncertainty evaluated from these cases.

2.3 Perfect and biased twin experiment setups

In this study, a perfect twin experiment framework and a biased twin experiment framework are designed, respectively. We first want to learn some basics from the perfect experiment which represents an idealized data assimilation regime. In the perfect twin experiment, both the assimilation model and "truth" model being used to produce "observations" use the standard parameter values listed in section 2.1, but they are started from different initial states. Then we use biased experiment setting to simulate the real world scenario in which the assimilation model has a systematic discrepancy from the observations. Thus, while the "truth" model uses the standard parameter values, the parameters including in the assimilation model will have 10% errors relative to the standard values. Here the errors in the parameters will be the only model error source. For the defined assimilation problem, the "truth" model using the standard parameter values is used to generate the "truth" solution of the models states and produce the observations sampled from the "truth". Starting from the initial condition (0,1,0,0,0), the "truth" model integrates forward 10000 TUs (1TU= $100\Delta t$) for sufficient spin-up and then integrates forward for another 10000TUs to generates the "truth" model states. The observations will be produced by sampling the "truth" solution of the model states at an observational interval and superimposing with a white noise simulating the observational error. As schematically shown in **Fig. 1**, all the observational intervals using in this study are assumed to be 1 time step (0.01TU). Based on that, **Fig. 1** also illustrates the assimilation update interval as well as the length of observational time window (OTW) etc. which will be used throughout the study. Although in the real climate system, the oceanic observations are usually available less frequently than those in the atmosphere (namely the ocean observational interval will be larger than that we set here), for this proof-of-concept study we will set the time interval of the oceanic observations as small as possible. The standard deviations of the observational errors are 2 for X_1, X_2, X_3 and 0.5 for ω. Also, although the deep ocean lacks observations in the real world, we also conduct some observation simulation experiments for η in this conceptual study.

In addition, the coupling strength between the atmosphere and ocean may have influences on the characteristic variability time scale of each coupled medium, so as on the optimal OTW. We discuss this issue through changing the values of coupling coefficients C_1 and C_2. In this simple model case, the coupling coefficient C_1 is sensitive to model stability (Zhang

Nonlin. Processes Geophys. Discuss., doi:10.5194/npg-2016-68, 2017
Manuscript under review for journal Nonlin. Processes Geophys.
Published: 13 January 2017
© Author(s) 2017. CC-BY 3.0 License.

et al., 2012) and only influences on the chaotic component, so here we just change C_2 to investigate the impact of coupling coefficient between the atmosphere and upper ocean on the optimal OTWs.

Same as Zhang and Anderson (2003), based on the results of a series of sensitivity tests on ensemble size, that of 20 is chosen in this study due to no significant improvement will obtain when using a larger one (Zhang and Anderson 2003; Zhang 2011a,b).

3 Observational time window length and retrieval of characteristic variability

3.1 Influence of observational time window on the accuracy of CDA

In order to exhibit the influence of OTW on the quality of climate analysis, we show 3 simple assimilation experiments (the absolute error of w) in **Fig. 2**: 1) standard CDA (green) (CDA with 0.05 TU atmosphere update interval and 0.2 TU ocean update interval), 2) OCN-OTW(5) CDA (red) (CDA with a 11 time step ocean OTW) and 3) OCN-OTW(100) CDA (CDA with a 201 time step ocean OTW). All assimilation experiments use a perfect model setting (all the parameters use their standard values) with a uni-variate adjustment scheme. While the standard CDA only assimilates the observations right at the assimilation time, the OCN-OTW CDA incorporates all the valid observations collected in the OTW. In the 3 assimilation experiments above, the atmosphere assimilation is identical – the assimilation interval is 0.05 TU with no OTW.

From **Fig. 2**, we can see that a small OCN-OTW (total 11 observations in the ocean OTW) can make a much better ocean analysis than the standard CDA (comparing the red line with the green line). We can understand that this is because an OTW can provide more observational information thus enhancing the observational constraint so as to improve the accuracy of climate analysis. However, comparing the blue line to the red line, it is clear that a too large OTW degrades the quality of the ocean analysis. The results of these simple assimilation experiments tell us, if an appropriate OTW is used, we can gain optimal climate analysis. How can we determine such an optimal OTW? Next, starting from analyzing characteristic variability of each coupled medium, we will discuss the methodology how to determine an optimal OTW for each medium in a coupled climate system.

3.2 The time scale of characteristic variability and optimal observational time window

The key to improve the accuracy of climate analysis in CDA is accurately recovering characteristic variability of different media in the coupled system. Thus we can assume that the length of optimal OTW for each medium will have some relationship with the corresponding characteristic variability time scale. Then, we should first analyze the time scale of characteristic variability in each medium.

Fig. 3 presents the power spectrum of , and based on the model states with a 4800-TU length (totally 4.8×105 data) after the spin-up described in section 2.3. From **Fig. 3**, we learned that in this simple model, the characteristic variability time scales of atmosphere ($\mathcal{X}_2$), upper ocean (ω) and deep ocean (η) are about 1-2 TUs, 50-100 TUs (5-10 model years) and 500

Nonlin. Processes Geophys. Discuss., doi:10.5194/npg-2016-68, 2017
Manuscript under review for journal Nonlin. Processes Geophys.
Published: 13 January 2017
© Author(s) 2017. CC-BY 3.0 License.

TUs (5 model decades), respectively. Namely, the characteristic variability time scale of the slab ocean is much larger than that of the atmosphere but smaller than that of the deep ocean.

An optimal OTW aims to provide maximal observational information that best samples characteristic variability of that medium during the data blending process. Thus the length of the optimal OTW should be smaller than the corresponding characteristic variability time scale, which means that the optimal OTW in the atmosphere must be much smaller than 1 TU (100 time steps), and in the ocean, the optimal OTW must be much smaller than 50 TUs (5000 time steps). If we will take observations for η, the optimal OTW for η must be much smaller than 500 TUs (50000 time steps).

From **Fig. 3**, we also see that the characteristic variability time scales of different coupled media are a little larger than the corresponding ones set in the Eq.(1). This is owing to the strong nonlinearity and smoothness of the fourth-order Runge-Kutta (RK4) time-differencing scheme that prolongs the characteristic variability time scales of the simple coupled model. But they do not change the essence of the problem we address in this study.

Given different time scales of characteristic variability in different media, in the following section we will further detect the optimal OTWs based on the corresponding characteristic variability time scale and examine their impact on the quality of climate analysis in CDA.

4 Detection of the optimal observational time window

In this section, with the perfect model framework described in section 2.3, we first conduct a series of CDA experiments with different ATM-OTWs and different OCN-OTWs to detect the optimal OTW for each medium. The assimilation scheme is the simple uni-variate adjustment scheme serving as a proof-of-concept study. To eliminate the dependency of results on initial states, each experiment is repeated for 20 independent initial conditions described in section 2.2. Then the mean value of 20 case RMSEs and the spread are plotted in **Fig. 4**.

Fig. 4a shows that the optimal ATM-OTW is 1, i.e., the optimal ATM-OTW includes only 3 atmosphere observations, with which the assimilation produces the lowest RMSE of the atmosphere and the smallest spread. In these experiments for detecting the optimal ATM-OTW, the ocean assimilation keeps in the standard setting (i.e. no OTW, 0.2 TU update interval). Then we keep the ATM-OTW as 1 and change the length of OCN-OTW to produce **Fig. 4b**.

From **Fig. 4b**, we can see that the optimal OCN-OTW is about 10 (i.e., each OTW includes total 21 observations), with which the lowest ω RMSE and the smallest RMSE spread are produced. Compared to the case of standard CDA (denoted as CDA_NOTW), the uses of optimal ATM-OTW and OCN-OTW make the RMSEs of $\mathcal{X}_{1,2,3}$ and ω significantly reduced. When the RMSE of ωhas a distinguishable convexity with respect to OCN-OTWs, the RMSE of $\mathcal{X}$ does not show such a sensitivity to the optimal OCN-OTW. This means that in this simple system, due to the strong nonlinearity and chaotic nature of the "atmosphere", the improved accuracy for ω from optimal observational constraint is not sufficient to impact the "atmosphere." This point will be discussed more in section 5.3. It is clear that when the OCN-OTW is larger than 25 (total 51 observations), the ω RMSE dramatically spread out throughout the cases, suggesting unstable CDA quality under the

Nonlin. Processes Geophys. Discuss., doi:10.5194/npg-2016-68, 2017
Manuscript under review for journal Nonlin. Processes Geophys.
Published: 13 January 2017
© Author(s) 2017. CC-BY 3.0 License.

circumstance. This is associated with too small ensemble spread causing filtering divergence (will be further discussed when we analyse the variation of ensemble spread with respect to the length of OTWs). Similar to the characteristic variability time scale of the slab ocean vs. that of the "atmosphere" shown by **Fig. 3**, the optimal OCN-OTW is much larger than that of ATM-OTW.

To further understand the relationship between the optimal OTW and characteristic variability time scale, we also examine the ηRMSEs in the space of η-OTWs. The assimilation interval of the pycnocline depth is set as 1 TU (100 time steps), which is much larger than that of the slab ocean. When we change the η-OTW, the optimal ATM-OTW and OCN-OTW detected from **Figs. 4ab** are used. As shown in **Fig. 4c**, the optimal η-OTW is about 100 (i.e. total 201 observations), which is much larger than that of OCN-OTW and smaller than the characteristic variability time scale of the deep ocean pycnocline depth. With the optimal η-OTW, the RMSE of η is reduced about 77.4% from the level of the CDA_NOTW.

We also check the variation of the 20-case mean ensemble spread in the space of OTWs as shown in **Fig. 5**. The mean and standard deviation of the ensemble spreads of $\mathcal{X}_{1,2,3}$ and ω gradually decrease when the ATM-OTW and OCN-OTW become larger. When the OTWs are set too large (here the ATM-OTW and OCN-OTW are greater than 20 and 250, respectively), the ensemble spreads of $\mathcal{X}_{1,2,3}$ and ω decrease dramatically. While increasing the length of the OTWs, more observations will be assimilated into the corresponding model states, which can function as a smoother. The larger the OTW is, the stronger the smoother is. Under this circumstance, the too strong smoother will distort characteristic variability of the model states, which explains the green line of **Fig. 2** as well as the dramatically large spread of RMSEs shown in **Fig. 4b**, when the OCN-OTW becomes larger than 25.

To understand the essence of optimal OTWs, we examine the auto-correlation for each model state. **Fig. 6** presents the auto-correlation coefficients of $\mathcal{X}_2$, ω and η in the space of lag times. The result is the mean of 20 cases. In each case, the number of data is 10000 (steps) (100TUs), which are chosen from the period of 5000TUs to 9000TUs in the truth run after spin-up. From **Fig. 6**, we learned that the complete de-correlation time scales of $\mathcal{X}_2$, ω and η are 0.27 TU, 16 TUs and 45 TUs respectively, much smaller than the corresponding characteristic variability time scales. We also learned the optimal OTWs detected from **Fig. 4** are much smaller than the de-correlation time scales. **Fig. 7** marks the time correlation coefficients at the time scales of optimal OTWs for $\mathcal{X}_2$ (panel a), ω (panel b) and η (panel c). We can see all are located around 0.995. This means that the observations including in an optimal OTW are extremely highly correlated with the model state at the analysis time. This can be understood since in this sequential assimilation scheme all the observations including in an OTW are assumed to be sampled at the analysis time so that the difference among them must be in a negligible arrange. Under such a circumstance, the optimal OTWs provide maximal observational information that best fits characteristic variability and minimizes the analysis error.

It is worth mentioning that although the essence of problem does not change with different assimilation algorithms, the length of the optimal OTW may be different when assimilation is implemented by different algorithms. For example, a 4-dimensional variational (4D-Var) scheme implements state estimation through minimizing a distance measure between the

Nonlin. Processes Geophys. Discuss., doi:10.5194/npg-2016-68, 2017
Manuscript under review for journal Nonlin. Processes Geophys.
Published: 13 January 2017
© Author(s) 2017. CC-BY 3.0 License.

model and observations defined on all individual observational times within an OTW. Since the minimized distance reflects the averaged effect in the OTW, obviously, if an inappropriate OTW is used, the estimated state also suffers distortion on its characteristic variability. However, unlike in the sequential scheme of this study, the difference among the observations in an OTW in a 4D-Var scheme is taken account into the minimized cost function to some degree. We can expect the optimal OTW in 4D-Var shall be larger than the one detected in this study but smaller than the corresponding de-correlation time scale. Detection of optimal OTWs in 4D-Var could be another research topic for follow-up studies, especially for an application in coupled data assimilation.

5 Influences of realistic assimilation scenarios on optimal OTW

In this section, we first show the impact of the multi-variate adjustment scheme on the optimal OTWs in perfect model setting. Then we discuss the influence of model bias through a biased model framework. We will also investigate the impact of coupling strength on the optimal OTWs.

5.1 Influence of multi-variate adjustment on optimal OTWs

While the experiments with the uni-variate adjustment scheme provide us a direct understanding of the influence of the OTWs on CDA, we want to check whether or not it also applies to the multi-variate adjustment scheme. So we repeat the experiments described in section 4 with the multi-variate adjustment scheme, and the gained results are shown in **Fig. 8**. Here the multi-variate adjustment scheme only limits to the atmospheric observations (i.e., only the cross-covariances among $\mathcal{X}_1, \mathcal{X}_2, \mathcal{X}_3$ are used) (as indicated in Han et al. 2013, the multi-variate adjustment scheme using the coupling cross-covariance between different coupled media involves complex scale interactions and may complicate the investigation of the problem we are addressing here). The results shown in **Fig. 8** are similar with **Fig. 4**, suggesting the multi-variate adjustment scheme has little influence on the optimal OTWs. This is because it does not change the characteristic variability time scales in this simple model.

The perfect experiment framework provides a direct guideline for the relationship between the optimal OTW and the corresponding characteristic variability time scale, as well as the impact on CDA. However, in reality, the numerical model has errors and is biased with the observation. It is necessary for us to investigate the influence of model bias on optimal OTWs so as on the quality of CDA.

5.2 Influence of model bias on optimal OTWs

With the biased model experiment framework described in section 2.3, we repeat all the experiments above for detection of the optimal OTWs. The results are shown in **Fig. 9**. Compared to the results in the perfect model setting, the results in the biased model setting have 2 differences. First, the optimal ATM-OTW and OCN-OTW are larger than their counterparts in the perfect model setting, becoming 3 and 20 (namely the total observations are 7 and 41, respectively). Second, the RMSE

Nonlin. Processes Geophys. Discuss., doi:10.5194/npg-2016-68, 2017
Manuscript under review for journal Nonlin. Processes Geophys.
Published: 13 January 2017
© Author(s) 2017. CC-BY 3.0 License.

curves in the space of OTWs show more convexity. This is more distinguishable in the curve of $\mathcal{X}_2$-RMSEs in the OCN-OTW space. All these phenomena can be explained by the influence of model bias on assimilation. Due to the existence of model bias, the assimilation not only needs observations to fit the observed variability but also needs observations to reduce the mean discrepancy between the model and observation. This requires stronger observational constraints. An optimal OTW that makes the smallest RMSE of model states must include more observed data. The test experiment for the optimal η-OTW is also consistent with this point (in **Fig. 9c**): the optimal η-OTW in the biased model setting is larger than the one in the perfect model setting. Then we also investigate the influence of OTWs on the quality of CDA with the multi-variate adjustment scheme in the biased experiment framework (not shown here). Conclusion is the same as the perfect model setting case, i.e., multi-variate adjustment scheme does not change the optimal OTWs.

Comparing the above two experiment frameworks, we can see that regardless of the perfect or biased model setting used in the assimilation experiments, the optimal OTW must be associated with the corresponding characteristic variability time scale in the medium. We found that the optimal OTW in the biased experiment framework is a little larger than that identified in the perfect experiment framework, since more observational information is needed to compensate the model bias and recover the characteristic variability. It is clear that while using observations in an OTW increases observational information, a too large OTW can distort the characteristic variability of coupled media during the information blending process. Therefore choosing an optimal OTW that is much smaller than the medium's characteristic variability time scale is very important. The simple model results suggest that the length of an optimal OTW is about 1-5% of the medium characteristic time scale, with which characteristic variability of the medium can be retrieved most accurately.

5.3 Influence of coupling strength on optimal OTWs

Changing coupling strength (controlled by the coupling coefficients $\mathcal{C}_1$and $\mathcal{C}_2$in this case) between the atmosphere and upper ocean may have some influence on the characteristic variability time scales of coupled media, so as on the optimal OTWs. Test experiments show that changing the coupling coefficient $\mathcal{C}_1$ has little influence on the characteristic variability time scales $\mathcal{X}_{1,2,3}$ and ω. This is because the characteristic time scale of $\mathcal{X}$ is determined by the chaotic nature of the Lorenz equations, not by the oceanic forcing associated with the coupling coefficient $\mathcal{C}_1$. Therefore, here we just change $\mathcal{C}_2$ to investigate the coupling coefficient between the atmosphere and upper ocean on the optimal OTW of ω. Setting the values of $\mathcal{C}_2$ as 1.5, 1.25, 1.0, 0.8, 0.5 and 0.1 and keeping $\mathcal{C}_1$ as 0.1, we repeat all the biased CDA experiments with the multi-variate adjustment scheme. The results are shown in **Fig. 10**, which presents the power spectrum of $\mathcal{X}_2$ and ω (panels ab) of six cases above based on the model states between 5000 TUs and 9800 TUs, as well as the time series of model states between 5000 TUs and 5100 TUs (panel c) after the spin-up described in section 2.3. We can see that changing $\mathcal{C}_2$ does not influence on the characteristic variability time scale of the atmosphere but strongly influences on variability of the slab ocean. From the equation of ω, the characteristic variability time scale of ω is determined by the combination of the atmospheric

Nonlin. Processes Geophys. Discuss., doi:10.5194/npg-2016-68, 2017
Manuscript under review for journal Nonlin. Processes Geophys.
Published: 13 January 2017
© Author(s) 2017. CC-BY 3.0 License.

forcing and the periodic external forcing. When $\mathcal{C}_2$ is small, the forcing of atmosphere to ocean is weak and then the periodic external forcing plays a dominant role on determining the characteristic variability time scale of ocean.

Then we examine the difference of the optimal OTW of ω in the above six cases, as shown in **Fig. 11**. Panels a and b show that changing $\mathcal{C}_2$ does not have any influence on the optimal ATM-OTW (all are about 3, i.e. totally 7 observations). From panel c and d, we can see that when $\mathcal{C}_2$ is smaller, the optimal OCN-OTW is larger. This can be explained by the increasing role of the periodic external forcing on determining variability of the slab ocean, for which data assimilation needs more observational information to recover the periodic variation of ω, determined by the time scale defined by $\mathcal{S}_{pd}$(10 TU). When $\mathcal{C}_2$ is larger than 1.0, changing it has little influence on characteristic variability of the ω, so as on the optimal OCN-OTW.

6 Summary and discussions

With a simple conceptual climate model and the EAKF method, the impact of OTWs on the quality of CDA has been investigated in this study. This simple conceptual coupled model consists of a synoptic atmosphere (Lorenz 1963) and seasonal-interannual slab upper ocean (Zhang et al. 2012) coupling with a decadal deep ocean (Zhang 2011a,b), and reasonably simulates the typical interactions between multiple time-scale components in the climate system. Determined from the characteristic variability time scale in each coupled medium, an optimal OTW provides maximal observational information to best fit characteristic variability of the medium during the data blending process. With correct scale interactions within the coupled system, CDA can recover the climate signals most accurately through incorporating all observations in the optimal OTWs into the coupled model. Although in an idealized and simple model circumstance, the conclusion addressing best fitting characteristic variability in each medium with the optimal OTW is comprehensive and therefore provides a guideline for improving climate analysis and prediction initialization when real observations are assimilated into a CGCM. For example, learned from the simple model results, we may consider to improve the quality of climate analysis and prediction initialization through accurately recovering some important characteristic variability in the atmosphere (sub-diurnal variations, for instance) and ocean (diurnal cycle in the tropical oceans, for instance).

However, the current work only can serve as a proof-of-concept study. Although CDA with the optimal OTWs has shown promising improvement in this simple model, serious challenges still exist for detecting optimal OTWs in the real world with a CGCM for improving climate analysis and predictions. First, the characteristic variability time scales in different media of the real world are complex and it remains great challenges to identify the characteristic variability of the different component models and the real atmosphere, upper and deep ocean, which need to be further studied. Also in a real ocean model, the upper and deep ocean are inseparable, which bring some troubles to use different OTWs for different parts of the same ocean mode. Second, due to model biases, characteristic variability in a CGCM may be different from the real world. The combination of variability of the real world and that of the model may further complicate the problem. Therefore, model bias and its influence on model variability need to be thoroughly analyzed before an optimal OTW is determined. In addition, in this study we assume that all observations in the OTWs have equal weighting to contribute to the observational constraint. In

© Author(s) 2017. CC-BY 3.0 License.

the real observation case, the observation far away from the assimilation time should have less contribution to the state estimation at the assimilation time. How to take the time correlation into account in a sequential algorithm and compare with the performance of 4D-Var needs to be studied before implementing optimal OTWs into the assimilation with CGCM and real observations.

Acknowledgements

Special thanks to Drs. Liwei Jia, Wei Zhang, Xuefeng Zhang, Wei Li, Lianxin Zhang, Shuo Yang for their comments and suggestions at the early version of this manuscript. This work was supported by the NSFC (No.51379049, 41676088), the Fundamental Research Funds for the Central Universities of China (No.HEUCFX41302, HEUCFD1505, HEUCF160410), the Young College Academic Backbone of Heilongjiang Province (No.1254G018), the Scientific Research Foundation for the Returned Overseas Chinese Scholars, Heilongjiang Province (No.LC2013C21) and China Scholar Council (awarded to Xiong Deng for two years' study abroad at UW-Madison – NOAA/GFDL Joint Visiting Program).

References

Anderson, J. L.: An ensemble adjustment Kalman Filter for data assimilation. Mon. Wea. Rev., 129, 2884-2903, doi:10.1175/15200493(2001)129<2884:AEAKFF>2.0. CO;2, 2001.

Anderson, J. L.: A local least squares framework for ensemble filtering. Mon. Wea. Rev., 131, 634-642, doi:10.1175/15200493(2003)131<0634:ALLSFF> 2.0.CO;2, 2003.

Anderson, J. L.: An adaptive covariance inflation error correction algorithm for ensemble filters. Tellus A, 59(2), 210-224, doi:10.1111/j.16000870.2006.00216.X, 2007.

Anderson, J. L.: Spatially and temporally varying adaptive covariance inflation for ensemble filter. Tellus A, 61(1), 72-83, doi:10.1111/j.16000870.2008.00361.X, 2009.

Chen, D., Zebiak, S. E., Busalacchi, A. J., and Cane, M. A.: An improved procedure for EI Nino forecasting: implications for predictability. Science, 269, 1699-1702, 1995.

Chen, D.: Coupled data assimilation for ENSO prediction. Adv. Geosci., 18, 45-62, 2010.

Collins, W. D., Blackman, M. L., Hack, J., Henderson, T. B., Kiehl, J. T., Large, W. G. and Mckenna, D. S.: The community climate system model version 3 (CCSM), J. Climate, 19, 2122-2143, doi:10.1175/JCLI3761.1, 2006.

Delworth, T. L., and Coauthors: GFDL's CM2 Global Coupled Climate Models. Part I: Formulation and simulation characteristics. J. Climate, 19(5), 643-674, doi:10.1175/JCLI3629.1, 2006.

Evensen, G.: Sequential data assimilation with a nonlinear quasi-geostrophic model using Monte Carlo methods to forecast error statistics. J. Geophys. Res., 99, 10143-10162, doi:10.1029/94JC00572, 1994.

Evensen, G.: Data assimilation: The Ensemble Kalman Filter. Springer, 187 pp, 2007.

© Author(s) 2017. CC-BY 3.0 License.

Gao, J., Xue, M. and Stensrud, D. J.: The development of a hybrid EnKF-3DVAR algorithm for storm-scale data assimilation. Advances in Meteorology, 2013, doi:10.1155/2013/512656, 2013.

Gnanadesikan, A.: A simple predictive model for the structure of the oceanic pycnocline. Science, 283, 2077-2079, 1999.

Hamill, T. M. and Snyder, C.: A hybrid ensemble Kalman filter-3D variational analysis scheme. Mon. Wea. Rev., 128(8), 2905-2919, doi:10.1175/15200493 (2000)128<2905:AHEKFV>2.0.CO;2, 2000.

Hamill, T. M., Whitaker, J. S. and Snyder, C.: Distance dependent filtering of background error covariance estimates in an ensemble Kalman filter. Mon. Wea. Rev., 129(11), 2776-2790, doi:10.1175/15200493(2001)129<2776:DDFOBE> 2.0.CO;2, 2001.

Han, G., Wu, X., Zhang, S., Liu, Z., and Li, W.: Error covariance estimation for coupled data assimilation using a Lorenz atmosphere and a simple pycnocline ocean model. J. Climate, 26(24), 10218-10231, doi: 10.1175/JCLI-D-13-00236.1, 2013.

Han, G., Zhang, X., Zhang, S., Wu, X. and Liu, Z.: Mitigation of coupled model biases included by dynamical core misfitting through parameter optimization: simulation with a simple pycnocline prediction model. Nonlinear Processes in Geophysics, 21, 357-366, doi:10.5194/npg-21-357-2014, 2014.

Houtekamer, P. L. and Mitchell, H. L.: Ensemble kalman filtering. Quarterly Journal of the Royal Meteorological Society, 131(613), 3269-3289, doi:10.1256/ qj.05.135, 2005.

Hunt, B. R., Kalnay, E., Kostelich, E. J. and Co-authors: Four-dimensional ensemble Kalman filtering. Tellus A, 56(4), 273-277, doi:10.1111/j.1600-0870. 2004.00066.x, 2004.

Kalman, R.: A new approach to linear filtering and prediction problems. Trans. ASME. Ser. D. J. Basic Eng. 82, 35-45, doi:10.1115/1.3662552, 1960.

Kalman, R. and Bucy, R.: New results in linear filtering and prediction theory. Trans. ASME. Ser. D. J. Basic Eng. 83, 95-109, doi:10.1115/1.3658902, 1961.

Laroche, S., Gauthier, P., Tanguay, M., Pellerin, S. and Morneau, J.: Impact of the different components of 4DVAR on the global forecast system of the Meteorological Service of Canada. Mon. Wea. Rev., 135(6), 2355-2364, doi:10. 1175/MWR3408.1, 2007.

Li, H., E. Kalnay, and Miyoshi, T.: Simultaneous estimation of covariance inflation and observation errors within an ensemble Kalman filter. Quart. J. Roy. Meteor. Soc., 135, 523-533, doi:10.1002/qj.371, 2009.

Lorenz, E. N.: Deterministic non-periodic flow. J. Atmos. Sci., 20, 130-141, 1963.

Miyoshi, T.: The Gaussian approach to adaptive covariance inflation and its implementation with the local ensemble transform Kalman filter. Mon. Wea. Rev., 139, 1519-1535, doi:10.1175/ 2010MWR3570.1, 2011.

Pires, C., Vautard, R. and Talagrand, O.: On extending the limits of variational assimilation in nonlinear chaotic systems. Tellus A, 48(1), 96-121, doi:10.1034/ j.1600-0870.1996.00006.x, 1996.

Randall, D. A., and Coauthors: Climate models and their evaluation. Climate Change 2007: The physical Science Basis, S. Solomon et al., Eds., Cambridge University Press, 589-662pp, 2007.

© Author(s) 2017. CC-BY 3.0 License.

Sugiura, N., Awaji, T., Masuda, S., Mochizuki, T., Toyoda, T., Miyama, T., Igarashi, H., Ishikawa, Y.: Development of a four-dimensional variation coupled data assimilation system for enhanced analysis and prediction of seasonal to interannual climate variations. J. Geophys. Res., 113(C10), C10017, doi: 10.1029/2008JC004741, 2008.

Whitaker, J. S. and Hamill, T. M.: Ensemble data assimilation without perturbed observations. Mon. Wea. Rev., 130, 1913-1924, doi:10.1175/1520-0493 (2002)130<1913:EDAWPO>2.0.CO;2, 2002.

Yang, X. and Coauthors: A predictable AMO-like pattern in GFDL's fully coupled ensemble initialization and decadal forecasting system. J. Climate, 26, 650-661, doi:10.1175/JCLI-D-12-00231.1, 2013.

Zhang, M., Zhang, F., Huang, X. Y. and Zhang, X.: Intercomparison of an ensemble Kalman filter with three-and four-dimensional variational data assimilation methods in a limited-area model over the month of June 2003. Mon. Wea. Rev., 139, 566-572, doi:10.1175/2010MWR3610.1, 2011.

Zhang, S. and Anderson, J. L.: Impact of spatially and temporally varying estimates of error covariance on assimilation in a simple atmospheric model. Tellus A, 55(2), 126-147, doi: 10.1034/j.1600-0870.2003.00010.x, 2003.

Zhang, S., Harrison, M. J., Rosati, A. and Wittenberg, A.: System design and evaluation of coupled ensemble data assimilation for global oceanic climate studies. Mon. Wea. Rev., 135, 3541-3564, doi: 10.1175/MRW3466.1, 2007.

Zhang, S.: Impact of observation-optimized model parameters on decadal predictions: simulation with a simple pycnocline prediction model. Geophys. Res. Lett., 38(L02702), 1-5, doi: 10.1029/2010GL046133, 2011a.

Zhang, S.: A study of impacts of coupled model initial shocks and state-parameter optimization on climate predictions using a simple pycnocline prediction model. J. Climate, 24(23), doi:10.1175/JCLI-D-10-05003.1, 2011b.

Zhang, S., Liu, Z., Rosati, A. and Delworth, T.: A study of enhancive parameter correction with coupled data assimilation for climate estimation and prediction using a simple coupled model. Tellus A, 64, 1-20, doi:10.3402/tellusa.v64i0. 10963, 2012.

Zhang, S., Winton, M., Rosati, A., Delworth, T., and Huang, B.: Impact of enthalpy-based ensemble filtering sea ice data assimilation on decadal predictions: simulation with a conceptual pycnocline prediction model. J. Climate, 26(7), 2368-2378, doi:10.1175/JCLI-D-11-00714.1, 2013.

Zhang, S., Chang, Y. –S., Yang, X., and Rosati. A.: Balanced and coherent climate estimation by combining data with a biased coupled model. J. Climate, 27(3), 1302-1314, doi:10.1175/JCLI-D-13-00260.1, 2014.

Nonlin. Processes Geophys. Discuss., doi:10.5194/npg-2016-68, 2017
Manuscript under review for journal Nonlin. Processes Geophys.
Published: 13 January 2017
© Author(s) 2017. CC-BY 3.0 License.

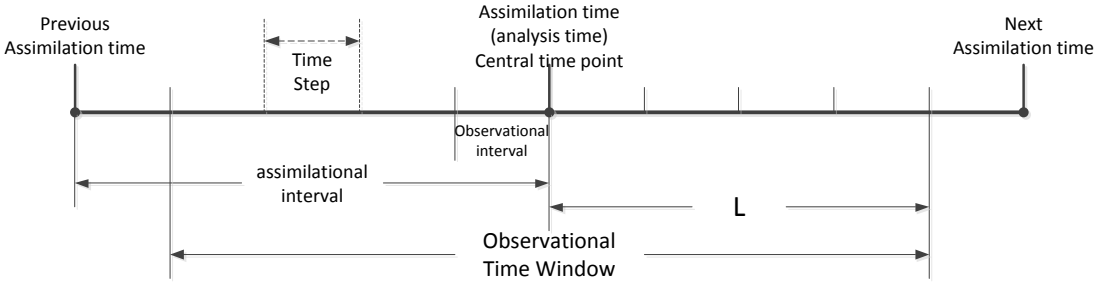

Figure 1: The schematic for the assimilation interval, the length of observational time window (OTW) as well as observational interval in terms of the model integration time step. Here L represents the time steps at one side of OTW. For example, OCN-OTW (L) in the content stands for an ocean observational time window with total observations of 2L+1.

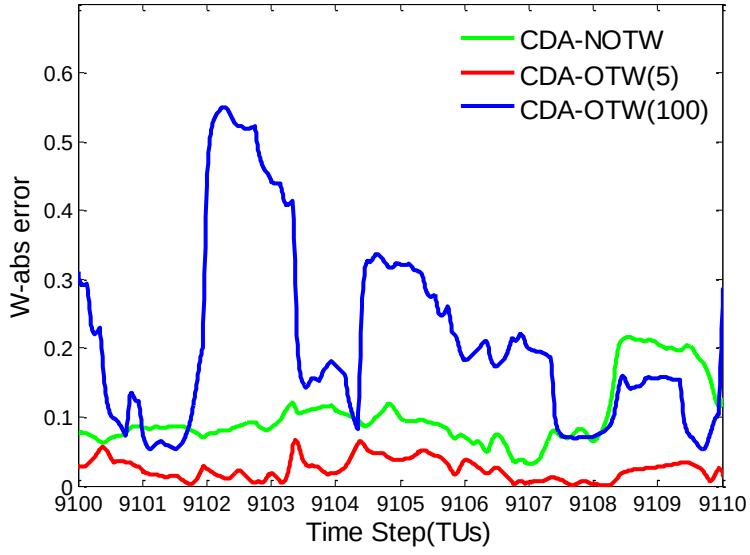

Figure 2: Time series of the absolute errors of the slab ocean variable (**ω**) in 3 assimilation experiments based on the model states between 9100 TUs and 9110 TUs assimilation results in the perfect model experiment framework with the uni-variate adjustment scheme. Green – CDA control with the standard update intervals of 0.05 TU for $\boldsymbol{\chi}_{1,2,3}$ and 0.2 TU for **ω**; Red – CDA with an ocean observational time window (OCN-OTW) of 5 time steps [OCN-OTW(5)]; Blue – CDA with OCN-OTW(100).

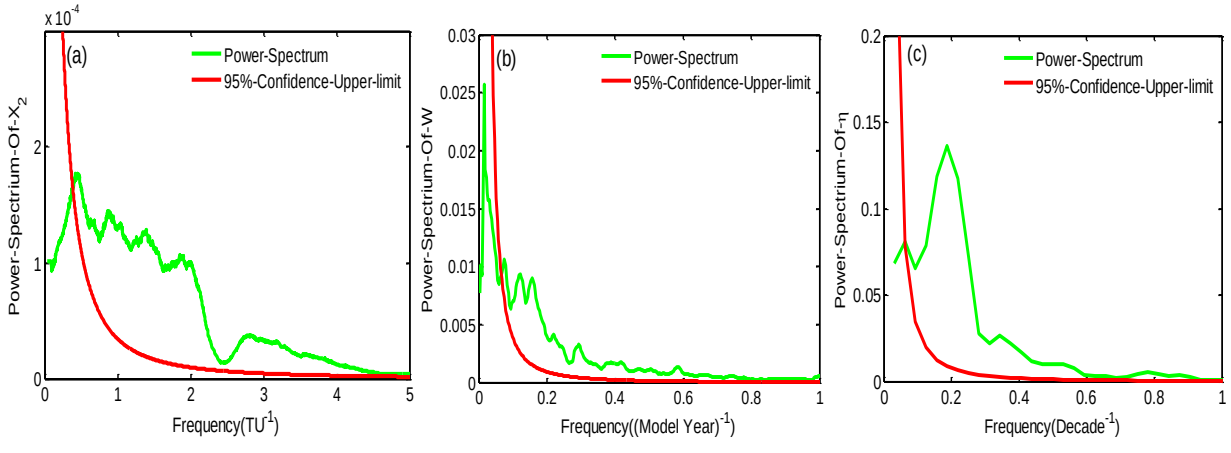

Nonlin. Processes Geophys. Discuss., doi:10.5194/npg-2016-68, 2017
Manuscript under review for journal Nonlin. Processes Geophys.
Published: 13 January 2017
© Author(s) 2017. CC-BY 3.0 License.

Figure 3: The power spectrum (green) of a) $\boldsymbol{X_2}$ b) **ω**, c) **η** based on the model states between 5000TUs and 9800TUs integrations after the spin-up which integrates for 10000TUs from the initial condition (0,1,0,0,0) with respect to the frequency, with 95% statistics significance (red).

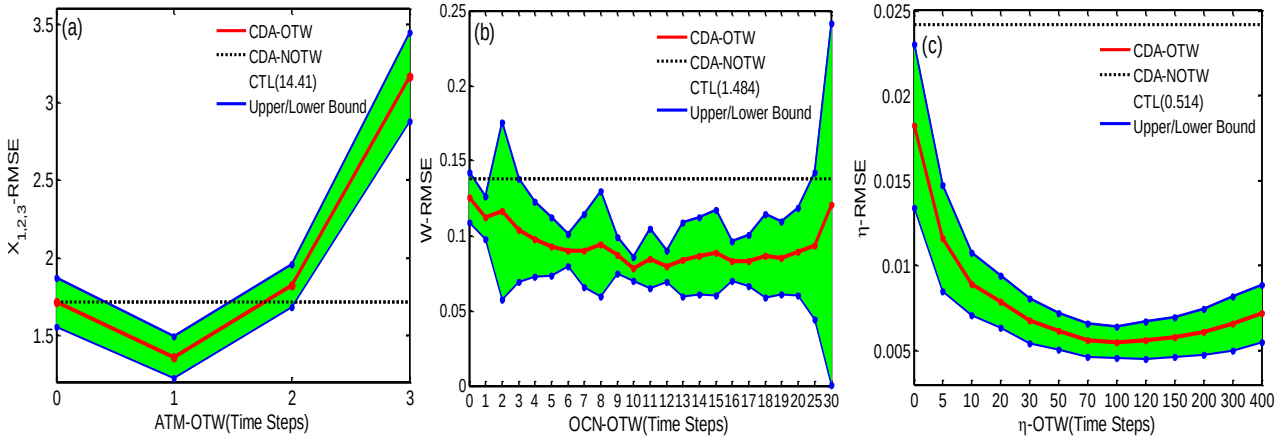

Figure 4: Variations of root mean square errors (RMSEs) of a) "atmospheric" states $\boldsymbol{X_{1,2,3}}$ (namely the average of $\boldsymbol{X_1}$, $\boldsymbol{X_2}$ and $\boldsymbol{X_3}$ RMSEs) in the space of ATM-OTW length when the "oceanic" state (**ω**) only uses a single observation at the assimilation time; b) "upper ocean" state (**ω**) in the space of OCN-OTW length when the ATM-OTW is fixed 1 as shown in panel a (1 for the ATM-OTW, i.e. 3 observations in each window, see the caption of Fig. 1) but the OCN-OTW (for **ω**) is varying and c) "deep ocean" state (**η**) in the space of **η**-OTW length when the "deep ocean" observations are assumed to be valid and the ATM-OTW and OCN-OTW are fixed as 1 and 10, respectively. The experiments are conducted in a perfect model setting with a simple uni-variate adjustment scheme. The red lines are the 20-case mean, each using different initial conditions taken from different periods in the control integration (see description in section 2.2), and the blue lines represent the upper/lower bounds (mean ± standard deviations) of the RMSEs. An OTW with the length of 0 represents only assimilating the observation at the assimilation time (i.e. with no OTW, dashed-black lines). The RMSE values of the control case (no observational constraint, called CTL) are marked in the parenthesis.

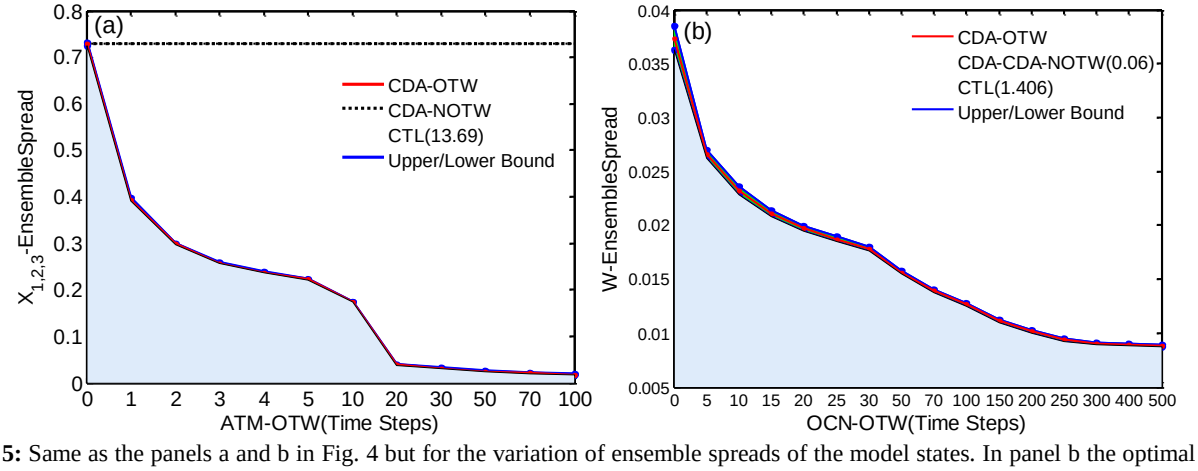

Figure 5: Same as the panels a and b in Fig. 4 but for the variation of ensemble spreads of the model states. In panel b the optimal ATM-OTW is also set as 1. The area between the lower and upper bounds (blue) represents the range evaluated from the 20 cases.

Nonlin. Processes Geophys. Discuss., doi:10.5194/npg-2016-68, 2017
Manuscript under review for journal Nonlin. Processes Geophys.
Published: 13 January 2017
© Author(s) 2017. CC-BY 3.0 License.

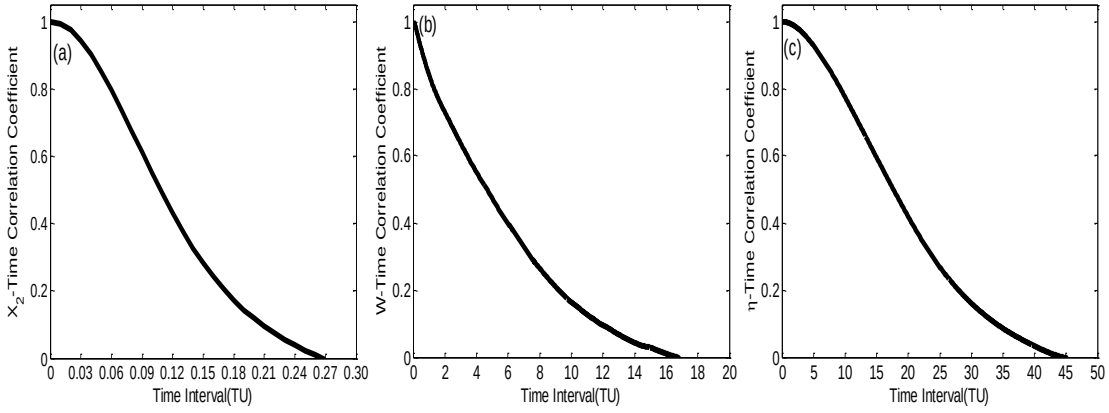

Figure 6: The auto-correlation coefficient of a) $\boldsymbol{\mathcal{X}_2}$ b) $\boldsymbol{\omega}$, c) $\boldsymbol{\eta}$ in the space of lag times. What are shown is the mean of 20 cases. In each case, an independent section (each has 10000 data of the state – 100 TUs with the interval of 0.01 TU) is used to evaluate the lag correlation coefficient. The 20 independent sections are taken from the model states apart each 200TUs between 5000TUs and 9000TUs integrations after the spin-up of 10000TUs from the initial condition (0, 1, 0, 0, 0).

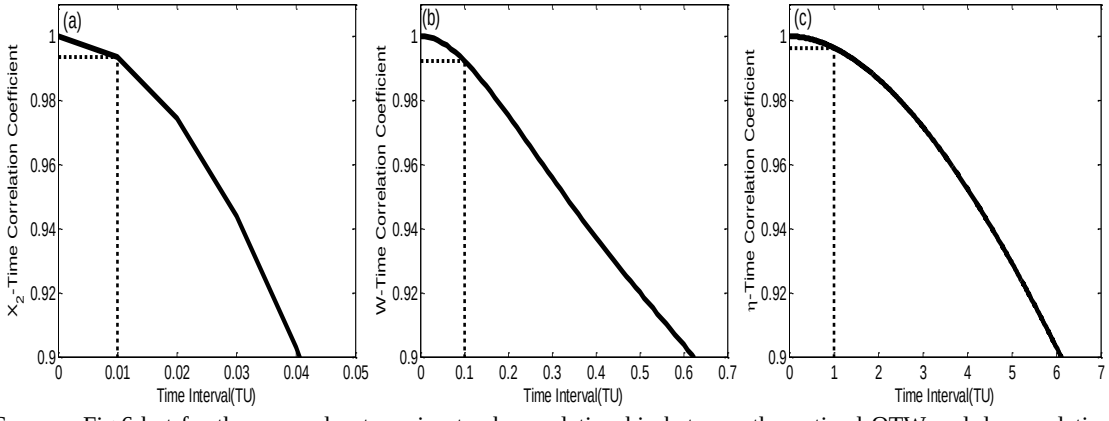

Figure 7: Same as Fig.6 but for the zoomed-out version to show relationship between the optimal OTW and de-correlation. The black dashed lines mark the corresponding time correlation coefficients at the time scale (L) of optimal OTWs as detected by Fig. 4 for different media.

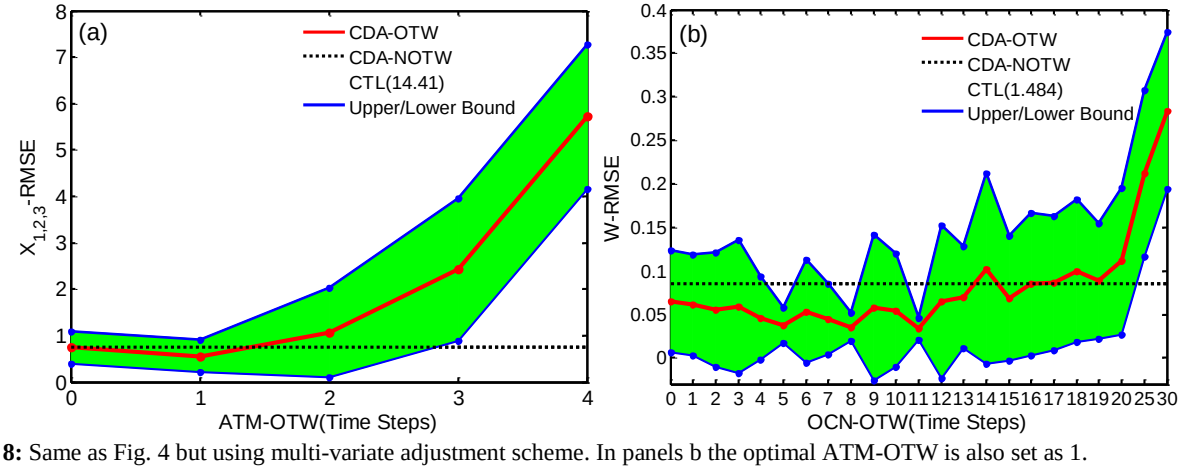

Figure 8: Same as Fig. 4 but using multi-variate adjustment scheme. In panels b the optimal ATM-OTW is also set as 1.

Nonlin. Processes Geophys. Discuss., doi:10.5194/npg-2016-68, 2017
Manuscript under review for journal Nonlin. Processes Geophys.
Published: 13 January 2017
© Author(s) 2017. CC-BY 3.0 License.

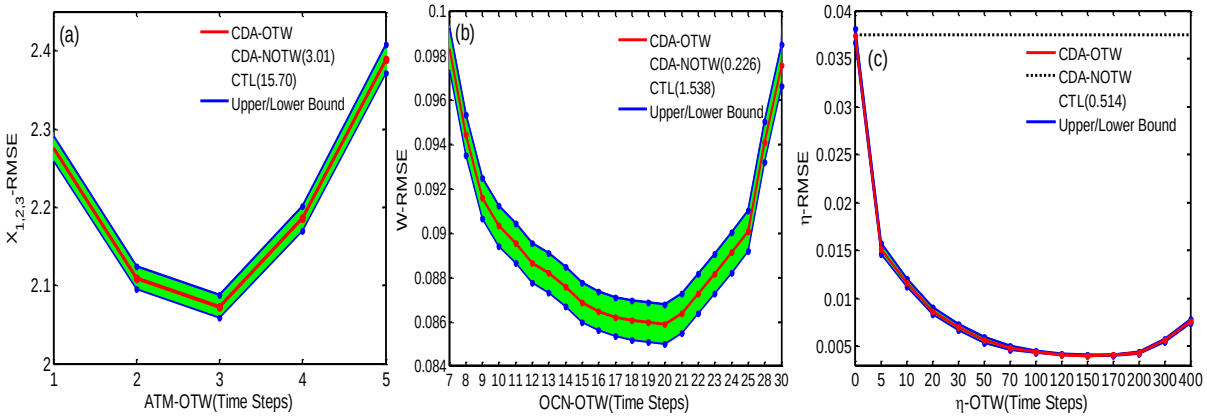

Figure 9: Same as Fig. 4 but using the biased model setting. In panels b) the optimal ATM-OTW is set as 3. And in panels c) the optimal ATM-OTW and OCN-OTW are kept as 3 and 20, when the "deep ocean" observations are assumed to be valid.

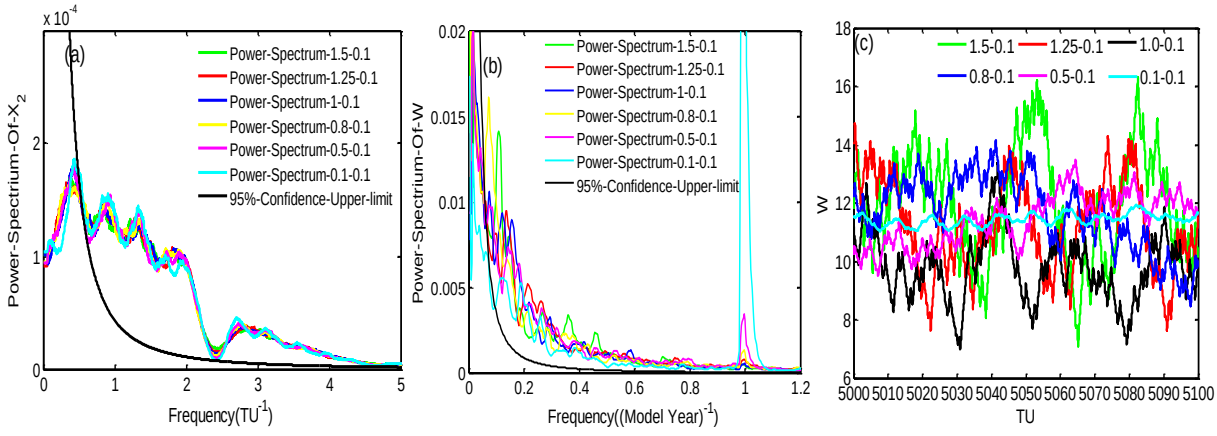

Figure 10: The power spectrum of a) $\boldsymbol{\mathcal{X}_2}$ and b) $\boldsymbol{\omega}$ based on the model states between 5000 TUs and 9800 TUs integrations after the spin-up which integrates for 10000TUs from the initial condition (0,1,0,0,0) with different coupling strength ($\boldsymbol{\mathcal{C}_2}$ is set as 1.5, 1.25, 1.0, 0.8, 0.5 and 0.1). Panel (c) shows the time series of the model state $\boldsymbol{\omega}$ between 5000 TUs and 5100 TUs integrations corresponding to the six cases.

Nonlin. Processes Geophys. Discuss., doi:10.5194/npg-2016-68, 2017
Manuscript under review for journal Nonlin. Processes Geophys.
Published: 13 January 2017
© Author(s) 2017. CC-BY 3.0 License.

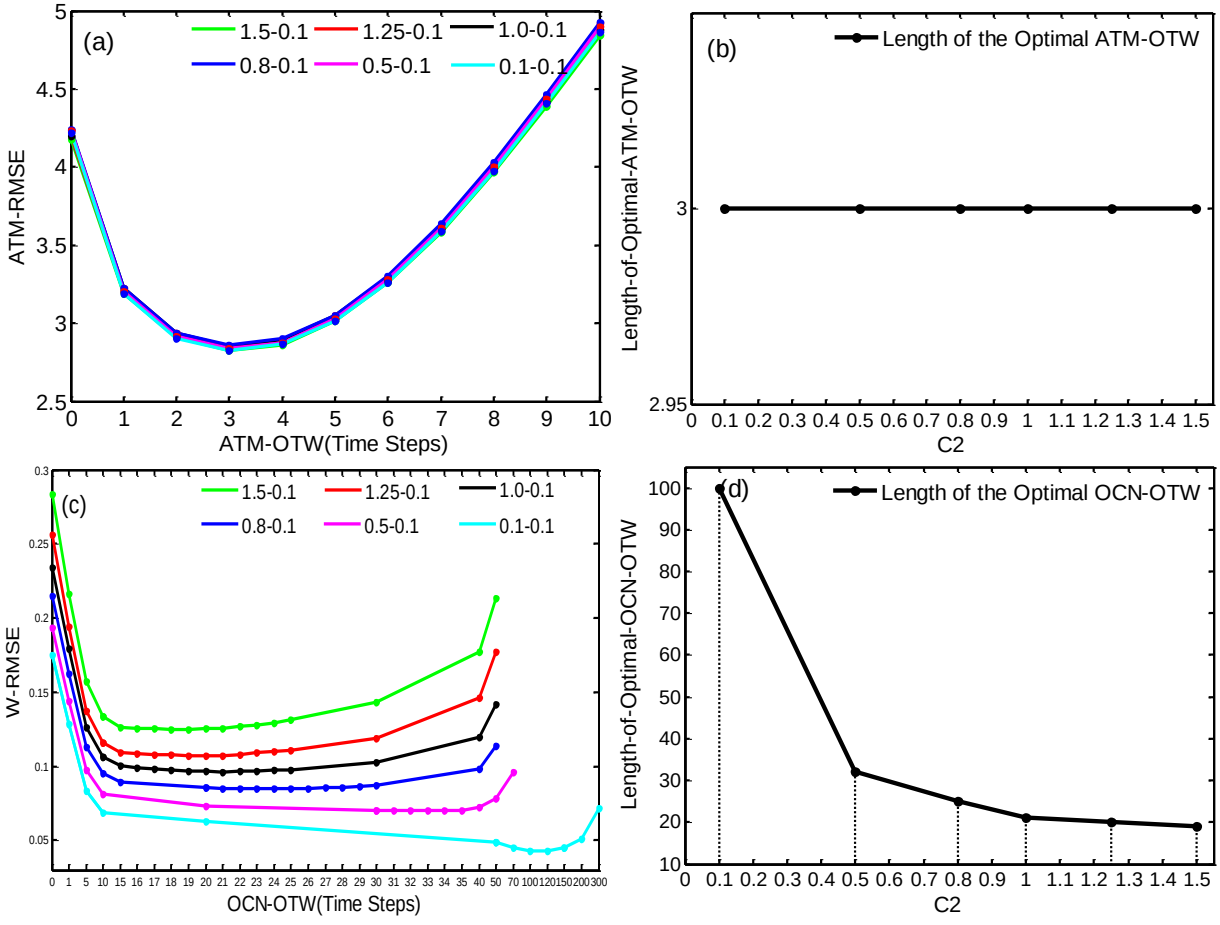

Figure 11: Panels a) and c) are the same as panels a) and c) in Fig. 7 but for cases using the biased model setting and six different coupling strength cases (with C_2 values as 1.5, 1.25, 1.0, 0.8, 0.5, 0.1). Panels b) and d) are the variation of the length of the optimal ATM-OTW and OCN-OTW with respect to the values of C_2.